Reactive state-space modelling of urban air pollution

V.V. Anh[1], M. Azzi[2], H. Duc[3], G.M. Johnson[2] and Q. Tieng[1]

[1]Centre in Statistical Science & Industrial Mathematics, Queensland University of Technology, GPO Box 2434, Brisbane, Q 4001, Australia.

[2]Division of Coal & Energy Technology, CSIRO, PO Box 136, North Ryde, NSW 3113, Australia.

[3] Environment Protection Authority of NSW, Locked Bag 1502, Bankstown, NSW 2200, Australia.

Abstract The generic reaction set (GRS) model offers a convenient framework for studying photochemical smog production. Its highly condensed seven equations are deduced from the principal reactions that produce photochemical smog (such as photolysis of reactive organic species, oxidation of NO to NO_2, photolysis of NO_2, etc.), and have been validated with CSIRO outdoor smog chamber data. The performance of the model has been found comparable to more detailed photochemical mechanisms such as the CBM-IV.
This paper expands the GRS model to include spatial advection and diffusion in the airshed. Via an appropriate numerical scheme, this extended dynamic model is transformed into the state space form, from which filtering and prediction can be performed using the Kalman algorithm. The model is implemented on a simple grid of seven stations in the Sydney monitoring network. One-step ahead forecasts are derived for observed as well as unobserved locations. Comparison with observed data indicate that the model performs reasonably well; in particular, it traces the ozone episodes accurately.

1 Introduction

Photochemical smog production is a complex process involving the reaction of reactive organic compounds (ROC), nitrogen oxides (NO_x) and sun light. In urban regions, under suitable meteorological conditions, these photochemical reactions can generate ozone concentrations which exceed public health standards. It is therefore essential for air quality management purposes to be able to predict the levels of ozone and other air pollutants ahead of time and at locations where there are no measurements.

Different kinetic mechanisms for photochemical smog have been proposed, some of which such as the CBM-IV of the UAM with 78 reactants and 170 reactions are very detailed. These models are commonly difficult to implement and require extensive computing resources. In contrast, the GRS model developed at the CSIRO Division of Coal & Energy Technology, Australia, is highly condensed and proves adequate as a practical means for the validation of airshed models which incorporate the GRS mechanism (Azzi, Johnson and Cope (1992), Hess *et al.* (1992)). It is deduced from the principal reactions that produce photochemical smog, and has been validated with CSIRO outdoor smog chamber data using a range of hydrocarbon mixtures and different ROC: NO_x ratios (see Hess *et al.* (1992) for a description of the CSIRO outdoor smog chambers). It has been found that GRS gives comparable or better performance than other photochemical mechanisms for conditions specified at the CSIRO outdoor smog chambers. In particular, the performance of GRS for the ROC:NO_x ratios characteristic of large Australian cities (population of 1-4 million) has been found to be far superior to that of CBM-IV,which appears to exhibit a systematic underprediction of the rate of smog formation for ratios of ROC:NO_x < 8ppm/ppmC (Cope and Ischtwan (1995)).

In this paper, we expand the GRS model to include spatial advection and diffusion in the airshed. Our purpose is to provide a dynamic space-time model which accommodates the main elements of air chemistry, advection, diffusion and emissions. It must be simple enough to be implemented on a personal computer, yet is capable of providing forecasts of pollution

concentrations over time and at unobserved locations comparable to those derived from more sophisticated models, such as the UAM.

The next section will recapture the elements of the GRS model. Section 3 will introduce advection and diffusion into the model via the established K theory. By using an appropriate numerical scheme, the extended model is transformed into the state space form, which then can be implemented via the Kalman filter. This is described in Section 4. For a demonstration, the model is implemented in Section 5 on a simple grid of 7 stations in the Sydney monitoring network. One-step ahead forecasts are derived and compared with observed values to evaluate the performance of the model. Some conclusions are then drawn in Section 6.

2 The GRS mechanism

The GRS mechanism has the following reactions

$$\begin{aligned} ROC + h\nu &\rightarrow RP + ROC; & RP + NO &\rightarrow NO_2 \\ NO_2 + h\nu &\rightarrow NO + O_3; & NO + O &\rightarrow NO_2 \\ RP + NO_2 &\rightarrow SGN; & RP + RP &\rightarrow RP \\ RP + NO_2 &\rightarrow SNGN, \end{aligned}$$

where ROC = reactive organic compound (NMHC and oxygenated products); RP = radical pool (lumped radical species); SGN = stable gaseous nitrogen product; SNGN = stable non-gaseous nitrogen product. The reaction rates for the above seven reactions are given by

$$\begin{aligned} R_1 &= k_1[ROC], & R_2 &= k_2[RP][NO], \\ R_3 &= k_3[NO_2], & R_4 &= k_4[NO][O_3], \\ R_5 &= k_5[RP][RP], & R_6 &= k_6[RP][NO_2], \\ R_7 &= k_7[RP][NO_2], \end{aligned}$$

It follows that, in the differential equation form,

$$\begin{aligned} \frac{d[RP]}{dt} &= k_1[ROC](t) - k_2[RP](t)[NO](t) \\ &\quad -k_5[RP]^2(t) - 2k_6[RP](t)[NO_2](t). \end{aligned} \quad (1)$$

Once $[NO](t), [NO_2](t)$ and $[ROC](t)$ are known, Eq. (1) can be solved for $[RP](t)$ using an efficient algorithm such as Milne's prediction-correction scheme. In order to determine $[ROC](t)$, we adopt the approach proposed by Johnson (1983) in his integrated empirical rate (IER) model, where $[ROC]$ is computed from the equation

$$\begin{aligned} &[NO](0) - [NO](t) + [O_3](t) - [O_3](0) = \\ &\quad 0.0067[ROC](t) + \int_{t_0}^{t} k_3 g(T(t))\, dt, \end{aligned} \quad (2)$$

$t_0 \equiv$ initial time of emissions and the air parcel, $g(T)$ is the temperature function defined above, with T now varying with time. Put

$$c^{(1)} = [O_3], \quad c^{(2)} = [NO], \quad c^{(3)} = [NO_2]. \quad (3)$$

Then, in view of the above analysis, the GRS model (in the differential equation form) is reduced to

$$\frac{dc^{(1)}}{dt} = k_3 c^{(3)}(t) - k_4 c^{(2)}(t) c^{(1)}(t), \quad (4)$$

$$\begin{aligned} \frac{dc^{(2)}}{dt} &= k_3 c^{(3)}(t) - k_4 c^{(2)}(t) c^{(1)}(t) \\ &\quad -k_2[RP](t) c^{(2)}(t), \end{aligned} \quad (5)$$

$$\begin{aligned} \frac{dc^{(3)}}{dt} &= k_2[RP](t) c^{(2)}(t) + k_2 c^{(2)}(t) c^{(1)}(t) \\ &\quad -k_3 c^{(3)}(t) - k_6[RP](t) c^{(3)}(t) - k_7[RP](t) c^{(3)}(t), \end{aligned} \quad (6)$$

where $[RP](t)$ is given by (1).

3 The extended GRS model

Under the assumptions of incompressible flow, isotropic horizontal turbulent diffusion and that molecular diffusion is negligible relative to turbulent diffusion, the K theory implies that the equations for conservation of mass in turbulent flows take the form

$$\begin{aligned} &\frac{\partial c^{(i)}}{dt} + u\frac{\partial c^{(i)}}{dx} + v\frac{\partial c^{(i)}}{dy} + w\frac{\partial c^{(i)}}{dz} = K_H\frac{\partial^2 c^{(i)}}{dx^2} + K_H\frac{\partial^2 c^{(i)}}{dy^2} \\ &+\frac{\partial}{\partial z}\left(K_V\frac{\partial c^{(i)}}{dz}\right) + r_i\left(c_1^{(1)}, c^{(2)}, c^{(3)}\right) + s^{(i)}(x,y,z,t) + d^{(i)}, \end{aligned} \quad (7)$$

$i = 1, 2, 3$, where $c^{(i)}$ is defined above, u, v, w are the x, y, z-components of wind speed, K_H is the horizontal diffusion coefficient, K_V is the vertical diffusion coefficient, r_i is the chemical reaction rate, $s^{(i)}$ is the emission inventory and $d^{(i)}$ is the deposition rate.

Eq. (7) can be written in a general form as

$$\frac{\partial c}{dt} + Lc = f \quad (8)$$

with the basic components:

$$\frac{\partial c}{dt} + Lc = 0, \quad \text{(advection \& diffusion)} \quad (9)$$

$$\frac{\partial c}{dt} = f \quad \text{(chemistry, source and sink).} \quad (10)$$

The system (10) consists of Eqs. (4) - (6). Define the operator L by

$$\begin{aligned} Lc^{(i)} &= -u\frac{\partial c^{(i)}}{dx} - v\frac{\partial c^{(i)}}{dy} - w\frac{\partial c^{(i)}}{dz} + K_H\frac{\partial^2 c^{(i)}}{dx^2} \\ &\quad +K_H\frac{\partial^2 c^{(i)}}{dy^2} + \frac{\partial}{\partial z}\left(K_V\frac{\partial c^{(i)}}{dz}\right), \quad i = 1, 2, 3. \end{aligned}$$

Then, in conjunction with (1) -(6), the extended GRS model of this paper is

$$\frac{dc^{(1)}}{dt} = Lc^{(1)} + k_3 c^{(3)}(t) - k_4 c^{(2)}(t) c^{(1)}(t), \quad (11)$$

$$\frac{dc^{(2)}}{dt} = Lc^{(2)} + k_3 c^{(3)}(t) - k_4 c^{(2)}(t) c^{(1)}(t) - k_2 [RP](t) c^{(2)}(t) + s^{(2)} + d^{(2)}, \quad (12)$$

$$\frac{dc^{(3)}}{dt} = Lc^{(3)} + k_2 [RP](t) c^{(2)}(t) + k_2 c^{(2)}(t) c^{(1)}(t) - k_3 c^{(3)}(t) - k_6 [RP](t) c^{(3)}(t) - k_7 [RP](t) c^{(3)}(t) + s^{(3)} + d^{(3)}, \quad (13)$$

4 The state-space form

Transforming an advection-diffusion equation into the state-space form was considered in Bankoff and Hanzevack (1975), Fronza *et al.* (1979), Hernandez *et al.* (1991). Following Fronza *et al.* (1979), we may consider an irregular grid for numerical approximations. The grid points on the x, y and z-axes are then denoted by

$$x_{l+1} = x_l + \Delta x_l, \quad l = 1, 2, ..., L,$$

$$y_{m+1} = y_m + \Delta y_m, \quad m = 1, 2, ..., M,$$

$$z_{n+1} = z_n + \Delta z_n, \quad n = 1, 2, ..., N;$$

in particular, ground level and mixing layer height correspond to $n = 1$ and $n = N$ respectively. The values $n = 0$ and $n = N + 1$ represent fictitious layers. In the discrete form, $c(x, y, z, t)$ is denoted by $c_{l,m,n}(t)$, where we have dropped the superscript i (for species i) for simplicity of notation as it is not needed until the final form for the entire system is considered. The boundary condition is then satisfied by setting

$$\Delta z_0 = \Delta z_1, \quad \Delta z_{N-1} = \Delta z_N,$$

$$K_0 = K_1, \quad K_{N+1} = K_N, \quad (14)$$

where $K = K_V$ in Eq.(7),

$$c_{l,m,0}(t) = c_{l,m,1}(t), \quad c_{l,m,N+1}(t) = c_{l,m,N}(t).$$

We also set

$$\Delta x_0 = \Delta x_1, \quad \Delta x_{L-1} = \Delta x_L,$$
$$\Delta y_0 = \Delta y_1, \quad \Delta y_{M-1} = \Delta y_M,$$
$$c_{0,m,n}(t) = c_{1,m,n}(t), \quad c_{L+1,m,n}(t) = c_{L,m,n}(t),$$
$$c_{l,0,n}(t) = c_{l,1,n}(t), \quad c_{l,M+1,n}(t) = c_{l,M,n}(t).$$

For a discrete approximation to (7), we may consider forward time difference to approximate time derivatives, second-order centered finite difference to integrate the advection and horizontal diffusion terms and the Crank-Nicholson method to integrate the vertical diffusion term. Defining the dimensionless coefficients:

$$\alpha_{l,m,n} = \frac{u_{l,m,n}\Delta t}{\Delta x_l + \Delta x_{l+1}}, \quad \beta_{l,m,n} = \frac{v_{l,m,n}\Delta t}{\Delta y_m + \Delta y_{m+1}},$$

$$\gamma_{l,m,n} = \frac{w_{l,m,n}\Delta t}{\Delta z_n + \Delta z_{n+1}},$$

$$\phi_l = \frac{K_H \Delta t}{\Delta x_{l+1}\Delta x_l}, \quad \psi_m = \frac{K_H \Delta t}{\Delta y_{m+1}\Delta y_m},$$

$$\theta_n = \frac{K_n \Delta t}{2\Delta z_{n+1}\Delta z_n}, \quad \pi_{n+1} = \frac{K_{n+1}\Delta t}{2\Delta z_{n+1}\Delta z_n},$$

a direct extension of the scheme given in Hernandez *et al.* (1991) to cover the case of inrregular grid yields

$$\begin{aligned} -\pi_{n+1} c_{l,m,n+1}(t+1) + \\ (1 + \pi_{n+1} + \theta_n) c_{l,m,n}(t+1) - \theta_n c_{l,m,n-1}(t+1) = \\ (1 - 2\phi_l - 2\psi_m - \pi_{n+1} - \theta_n) c_{l,m,n}(t) + \\ (\phi_l - \alpha_{l,m,n}) c_{l+1,m,n}(t) + \\ (\phi_l + \alpha_{l,m,n}) c_{l-1,m,n}(t) + \\ (\psi_m - \beta_{l,m,n}) c_{l,m+1,n}(t) \\ + (\psi_m + \beta_{l,m,n}) c_{l,m-1,n}(t) + \\ (\pi_{n+1} - \gamma_{l,m,n}) c_{l,m,n+1}(t) + \\ (\theta_n + \gamma_{l,m,n}) c_{l,m,n-1}(t) + \\ [r_{l,m,n}(t) + s_{l,m,n}(t) + d_{l,m,n}(t)] \Delta t. \end{aligned} \quad (15)$$

Eq. (15) can be put in a vector form by defining

$$c(t) = vec(c_{l,m,n}(t))_{l=1,...,L,\, m=1,...,M,\, n=1,...,N}.$$

We then get (15) being equivalent to

$$Dc(t+1) = Ec(t) + F, \quad (16)$$

where D is a matrix of $N \times N$ blocks, each block being a zero matrix or a diagonal matrix of size $LM \times LM$, E is a matrix obtained from the right hand side of (15), and

$$F = vec((r_{l,m,n}(t) + s_{l,m,n}(t) + d_{l,m,n}(t)) \Delta t),$$

$$l = 1, ..., L, \quad m = 1, ..., M, \quad n = 1, ..., N.$$

We mainly consider $N = 2$. Then, it can be derived that

$$D = \begin{bmatrix} (1 + \pi_2) I & -\pi_2 I \\ -\theta_2 I & (1 + \theta_2) I \end{bmatrix},$$

I being the identity matrix of size $LM \times LM$. Being decomposed into blocks of zero or diagonal matrices,

the inverse of D always exists and is easy to compute. Eq. (16) will then be written as

$$c(t+1) = A\,c(t) + B, \tag{17}$$

where

$$A = D^{-1}E, \quad B = D^{-1}F.$$

We can now introduce a noise term into the state equation (17) and an observation equation. The model is then in the state-space form:

$$\begin{cases} c(t+1) = A\,c(t) + B + \varepsilon(t), \\ y(t) = H\,c(t) + u(t), \end{cases} \tag{18}$$

where $y(t)$ is the vector of concentrations observed at the sites, H is a matrix whose elements are either 0 or 1, the value 1 corresponding to a grid point coinciding with a site,

$$E\left(\varepsilon(t)\ \varepsilon'(t+k)\right) = \begin{cases} Q(t), & k=0, \\ 0, & k \neq 0, \end{cases}$$

$$E\left(u(t)\ u'(t+k)\right) = \begin{cases} R(t), & k=0, \\ 0, & k \neq 0. \end{cases}$$

The covariance matrix $Q(t)$ of the state equation is taken to have the form

$$Q_{ij}(t) = E\left(\varepsilon_i(t)\,\varepsilon_j(t)\right) = \frac{r_{ij}}{2\alpha} K_1(\alpha r_{ij}), \tag{19}$$

where r_{ij} is the distance between site i and site j on the grid, and K_1 is the modified Bessel function of the second kind, order 1. The form (19) is deduced from the atmospheric diffusion equation of the K theory (Anh *et al.* (1997)). Nonlinear least squares fitting to the cumulative semivariogram of monthly averaged ozone data at 18 monitoring stations of the Sydney region yields that $\widehat{\alpha} = 0.148$ for the period under study (January 1994). The form (19) seems adequate in representing the spatial variability of a homogeneous and isotropic concentration field (Anh *et al.* (1997)).

The covariance matrix $R(t)$ of the observation equation is set at the values

$$R_{ij}(t) = \begin{cases} 0.1, & i=j \\ 0, & i \neq j \end{cases} \tag{20}$$

to reflect moderate random errors in the measurements.

System (18) is derived for a species $c^{(i)}$. The complete system for $c^{(1)}, c^{(2)}$ and $c^{(3)}$ can now be written in the form (18) with

$$c = \left[c^{(1)}\ c^{(2)}\ c^{(3)}\right], \qquad B = [B_1\ B_2\ B_3]^T,$$
$$\varepsilon = [\varepsilon_1\ \varepsilon_2\ \varepsilon_3]^T, \qquad u = [u_1\ u_2\ u_3]^T,$$

$$A = \begin{bmatrix} A_1 & 0 & 0 \\ 0 & A_2 & 0 \\ 0 & 0 & A_3 \end{bmatrix}, \quad H = \begin{bmatrix} H_1 & 0 & 0 \\ 0 & H_2 & 0 \\ 0 & 0 & H_3 \end{bmatrix},$$

T denoting the transpose of a matrix. Since there is no change in the notation, we shall continue to use (18) to denote this complete system.

The Kalman algorithm for filtering and prediction of system (18) is

$$\begin{aligned} c(t|t) &= c(t|t-1) \\ &\quad + G(t)\left(y(t) - H\,c(t|t-1)\right), \\ c(t+1|t) &= A\,c(t|t) + B, \\ G(t) &= P(t|t-1)\,H' \\ &\quad \times \left(H\,P(t|t-1)\,H' + R(t)\right)^{-1}, \\ P(t|t) &= (I - G(t)\,H)\,P(t|t-1), \\ P(t+1|t) &= A P(t|t)\,A' + Q(t+1) \end{aligned}$$

where $c(t|t)$ is the estimation of $c(t)$ based on the new data $y(t)$, $c(t+1|t)$ is the prediction of $c(t+1)$ made at time t, $G(t)$ is the Kalman gain, which gives a correction to the previous forecast $c(t|t-1)$, and $P(t|t-1)$ is the covariance matrix of the prediction error, which is recursively computed through the last two equations of the algorithm (see Brockwell and Davis, 1991, for example, for the derivation of this algorithm).

Remark 1 *The system (18) for the three species $c^{(1)}, c^{(2)}$ and $c^{(3)}$ is much more complex than those considered in Bankoff and Hanzevac (1975), Fronza et al. (1979), and Hernandez et al. (1991). In these latter studies, the state-space form was obtained for a single species, while our system (18) allows for reactive relationships between the three species of (3). These relationships connect and describe the reactive dynamics of the individual equations of the system. The Kalman algorithm also offers a convenient framework for experimenting and seeing the influence of different effects on the generation of $c^{(1)}, c^{(2)}$ and $c^{(3)}$. For example, under suitable conditions such as calm days with strong sunlight, the chemistry part (mainly the matrix B in (18)) will be dominant in the algorithm. On the other hand, under other meteorological conditions such as days with strong wind, advection and diffusion transport will take effect while the chemical reaction rates become close to zero yielding the term B insignificant in the algorithm (apart from some adjustments for emissions and deposition rates).*

5 Experimental results

We consider two examples of the Sydney monitoring network:

(i) The grid consisting of six stations: St Marys, Blacktown, Westmead, Lidcombe, Liverpool and Bringelly;

(ii) The grid consisting of seven stations: St Marys, Blacktown, Westmead, Lidcombe, Liverpool, Bringelly and Campbelltown;

The location of these stations in the Sydney network (of 18 monitoring stations) is given in Figure 1. The domain under consideration is urban. We shall use the values measured on 9 January 1994 as a test case, which is characterised by moderate concentrations of ozone in south-west Sydney. We shall consider only two levels: ground level and the mixing height level (maximum 2000m above ground level). Hence for example (i), which is considered as a rectangular grid with $L = 3, M = 2, N = 2$. The values of the wind field used in this study are the observed values at the above locations.

The diffusivity coefficients are computed as

$$K_H(l,m,n) = 0.216\, w_* h, \tag{21}$$

$$K_V(l,m,n) = K_H(l,m,n), \tag{22}$$

where w_* is the convective velocity scale and h is the mixing height. The constant 0.216 of (21) and the estimates of w_* are obtained from the CSIRO Lagrangian atmospheric dispersion model (LADM), which is an air pollution dispersion model simulating the transport and diffusion of emissions of pollutants from discrete sources. It has a prognostic windfield component and a Lagrangian particle dispersion component (see Physick *et al.*, 1994). The mixing height h is estimated using the diagnostic equations as reported in Duc and Lashmar (1996). For the period under study, the neutral and stable conditions prevailed at night time according to the windspeed classification, while an unstable condition was observed during the day.

Due to lack of reliable data on emissions and deposition rates, we follow Fronza *et al.* (1979) in heuristically correcting these values through an *a posteriori* pollutant mass balance, which is effected from a comparison between filtered and previously predicted overall mass of pollutants at ground level.

The filtering and prediction of O_2, NO, NO_2 and RP is carried out in an iterative fashion:

(a) The values of $[O_3](t), [NO](t)$ and $[NO_2](t)$ obtained from the Kalman filter for system (18) are used in (2) to get $[ROC](t)$. These estimates are then included in (1) and the equation is solved for $[RP](t)$.

(b) The solution $[RP](t)$ of (1) is used in (18) to obtain the next estimates of $[O_3](t), [NO](t)$ and $[NO_2](t)$ from the Kalman filter. Go to Step (a).

The algorithm is applied to grid (i), and one-step ahead forecasts are derived for each station. As a typical example, the predicted and observed ozone values at Bringelly are presented in Figure 2. The exercise is repeated for grid (ii), where Campbelltown is added to grid (i); but in this exercise, we assumed that there were no measurements at Campbelltown. The Kalman predictor was then activated based on information at the other six sites of the grid and produced one-step ahead forecasts for Campbelltown. The forecasts for Campbelltown are displayed in Figure 3.

6 Conclusions

This paper expands the GRS photochemical model into a dynamic space-time model which accommodates the main elements of air chemistry, advection, diffusion and emissions. This extended model is then put into the state-space form using appropriate stable numerical schemes which allow for irregular grids, a common feature of monitoring networks. The covariance structure of the noise term of the state equation reflects the spatial variability of the Sydney airshed established in a previous study. Another important contribution of the paper is the modelling of the reactive dynamics of three key species (O_3, NO, NO_2) of photochemical smog within a state-space framework. It should be noted that previous state-space models concentrated on a single species, hence were not concerned with reactive relationships between the species, which is a key aspect of photochemical smog production. Due to its reasonably compact size and the fast Kalman algorithm, the model offers a needed tool for experimentation and scenario analyses, particularly for investigating the effect of different meteorological conditions on the generation of O_3, NO, NO_2. Numerical results on a grid of seven stations indicate that the performance of the model is quite creditable in terms of producing ozone forecasts for an unobserved location, which is a difficult but important task of airshed modelling. Work is being undertaken to evaluate the model on a more extensive grid of the Sydney region.

References

[1] Anh, V.V., Duc, H. and Shannon, I., Spatial variability of Sydney air quality by cumulative semivariogram, Atmospheric Environment (to appear).

[2] Azzi, M., Johnson, G.M. and Cope, M., An introduction to the generic reaction set photochemical smog mechanism, Proc. 11th International Conf. of the Clean Air Society of Australia & New Zealand, Brisbane, 1992.

[3] Bankoff, S.G. and Hanzevack, E.L., The adaptive-filtering transport model for prediction and control of pollutant concentration in an urban airshed, Atmospheric Environment 9(1975), 793-808.

[4] Brockwell, P.J. and Davis, R.A., Time Series: Theory and Methods, Springer-Verlag, New York, 1991.

[5] Cope, M. and Ischtwan, J., Appendices to March'95 Draft Report on Metropolitan air quality study airshed modelling. Environment Protection Authority of NSW, June 1995.

[6] Duc, H. and Lashmar, M., Estimate of mixing height using surface meteorological data, Proc. Clean Air Society of Australia & New Zealand, Adelaide, 1996.

[7] Fronza, G., Spirito, A. and Tonielli, A., Real-time forecast of air pollution episodes in the venetian region. Part 2: The Kalman predictor, Appl. Math. Modelling 3(1979), 409-415.

[8] Hernandez, E., Martin, F. and Valero, F., State-space modelling for atmospheric pollution, J. Applied Meteorology 30(1991), 793-811.

[9] Hess, G.D., Carnovale, F. Cope, M. and Johson, G.M., The evaluation of some photochemical smog reaction mechanisms-I. Temperature and initial composition effects, Atmospheric Environment 26A(1992), 625-641.

[10] Johnson, G.M., An empirical model of photochemical smog formation, Proc. 6th World Congress on Air Quality, Vol. 1, IUAPPA, Paris, 1983, pp. 25-32.

[11] Physick, W., Noonan, J.A., McGregor, J.L., Hurley, P.J., Abbs, D.J. and Manings, P.C., LADM: A Lagrangian Atmospheric Dispersion Model, CSIRO Division of Atmospheric Research Technical Paper No. 24, 1994.

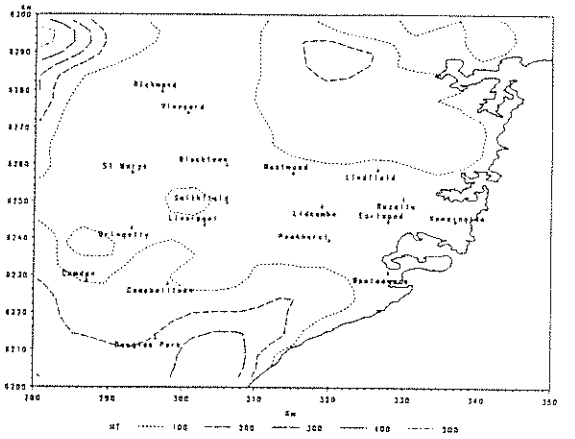

Figure 1. The air quality monitoring network of the Sydney region

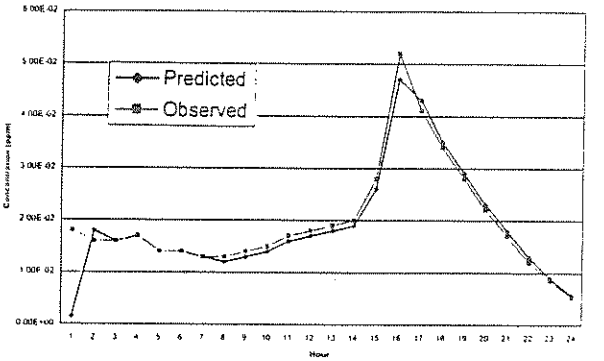

Figure 2. Predicted and observed ozone at Bringelly

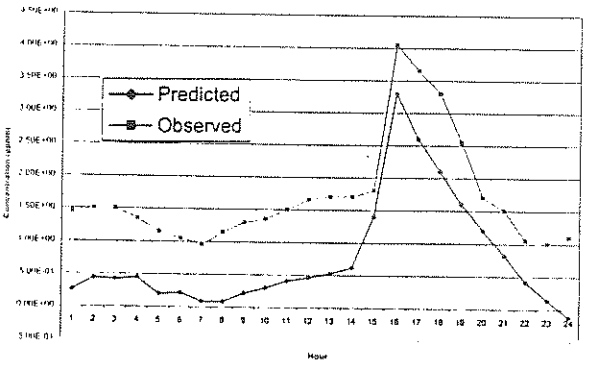

Figure 3. Predicted and observed ozone at Campbelltown